α- and β-Stilbenosides as base-pair surrogates in DNA hairpins†

Ligang Zhang,[a] Hai Long,[a] Grant E. Boldt,[b] Kim D. Janda,*[b] George C. Schatz[a] and Frederick D. Lewis*[a]

Received 6th October 2005, Accepted 10th November 2005
First published as an Advance Article on the web 8th December 2005
DOI: 10.1039/b513694f

The synthesis, structure, and optical spectroscopy of hairpin oligonucleotide conjugates possessing synthetic stilbene C-nucleosides (stilbenosides) are reported. Synthetic methods for selective preparation of both the α- and β-stilbenosides have been developed. Both anomers are effective in stabilizing hairpin structures when used as capping groups at the open end of the hairpin base-pair domain. However, only the β-anomer effectively stabilizes the hairpin structure when located in the interior of the base-pair domain opposite an abasic site. Similar results are obtained for hairpins possessing two stilbenosides, either adjacent to each other or with one intervening base-pair. Molecular dynamics simulations are employed to obtain averaged structures for these conjugates. The calculated structures for the capped hairpins formed with either anomer show effective π-stacking with the adjacent base-pair. The calculated structures for the internal stilbenosides show that the α- and β-anomers form extrahelical and intrahelical structures, respectively. The relative orientations of the two stilbenes in the bis-stilbenosides have been studied using a combination of exciton-coupled circular dichroism spectroscopy and molecular modeling.

Introduction

Aromatic π–π interactions are an important contributing factor to the stabilization of duplex DNA.[1] The aromatic stacking abilities of synthetic β-nucleosides possessing non-natural aromatic bases have been extensively investigated by Kool and co-workers.[2] They report that the stability of self-complementary duplexes possessing dangling synthetic β-nucleosides increases as the surface area of the adjacent base-pair covered by the arene increases (benzene < naphthalene < phenanthrene < pyrene).[3] These workers also investigated the thermal stability of duplexes possessing the β-pyrenoside **β-Py** opposite an abasic site **X** (Chart 1) within the interior of a 12-mer duplex.[4,5] These duplexes proved to be slightly more stable than a reference duplex lacking this base-pair, but less stable than a duplex possessing an A:T base-pair in place of the **β-Py**–**X** base-pair surrogate.

The dimensions of the conjugated aromatic *trans*-stilbene provide an excellent match for those of the purine–pyrimidine base-pairs. Thus stilbene nucleosides (stilbenosides) might serve as effective base-pair surrogates and also serve as intrinsic fluorescent probes of the duplex interior. We and others have reported that the stilbenedicarboxamide **Sa** (Chart 1) and other stilbene derivatives can serve as capping groups for duplexes and hairpins and as hairpin linkers in a variety of oligonucleotide conjugates.[6–10] In the conjugates investigated to date, the stilbene is attached to the oligonucleotide by means of short, flexible tethers. This permits the stilbene to be positioned at the end of a duplex base-pair domain, but not in the interior. Synthetic nucleosides can be positioned either at the end or within the interior of the base-pair domain. The synthesis of the α-anomer of a stilbene C-nucleoside linked at the stilbene *para* position has been reported by Strässler *et al.*;[11] however it has not been incorporated into an oligonucleotide conjugate. Neither has a comparative study of aromatic α- *vs.* β-C-nucleosides been reported.

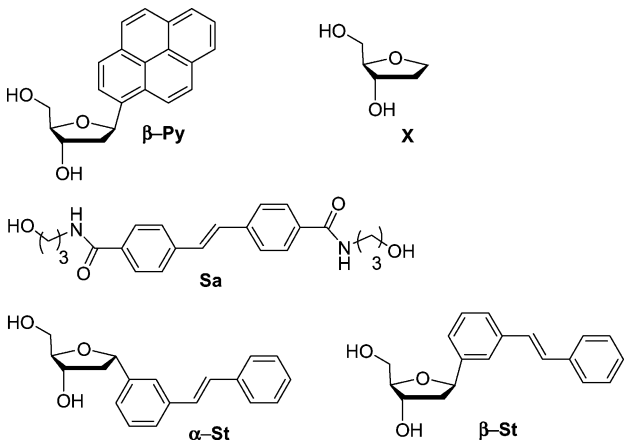

Chart 1

Molecular modeling of the isomeric stilbenosides suggested that the *meta* isomers might provide more complete coverage of the adjacent base-pairs without deformation of the sugar–phosphate backbone of B-DNA than would the *para* isomers. Thus we have undertaken the synthesis of the anomeric stilbenosides **α-St** and **β-St** (Chart 1) and several hairpin-forming conjugates in which one or two stilbenosides are located either at the end or opposite an abasic site within the interior of a short base-pair duplex domain (Chart 2). We report here the results of our investigation of the synthesis, structure, and optical spectroscopy of these conjugates. Both stilbenoside anomers can function as capping groups but

[a]*Department of Chemistry, Northwestern University, Evanston, IL, 60201. E-mail: lewis@chem.northwestern.edu*
[b]*Departments of Chemistry and Immunology and The Skaggs Institute for Chemical Biology, The Scripps Research Institute, 10550, N. Torrey Pines Road, La Jolla, CA, 92037. E-mail: kdjanda@scripps.edu*

† Electronic supplementary information (ESI) available: HPLC and MALDI TOF mass spectra for conjugates. Averaged truncated structures for **8**β and **9**β. Partial atomic charges and atom types for the stilbenosides used in MD simulations. See DOI: 10.1039/b513694f

 This journal is © The Royal Society of Chemistry 2006

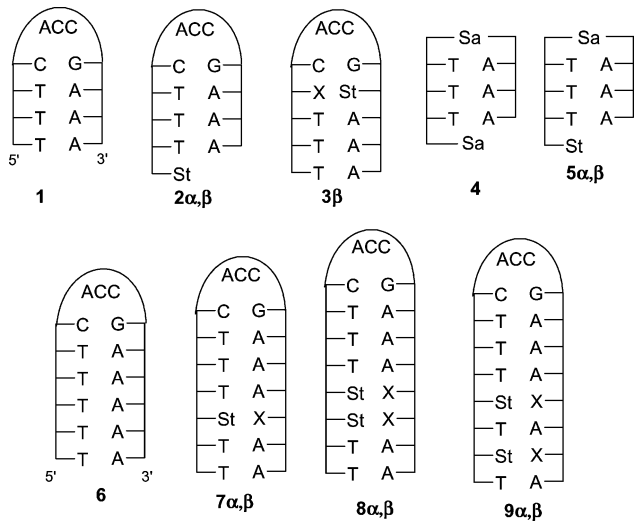

Chart 2

only the β-anomer forms stable conjugates with an intrahelical stilbenoside structure. Studies of the hairpin thermodynamic stability indicate that the β-**St** nucleoside is comparable to β-**Py** in its ability to stabilize duplex structures either as a dangling end-capping nucleoside or opposite an abasic site within the duplex interior. The strong electronic transition dipoles of the stilbene chromophores permits the study of the relative orientation of two intrahelical stilbenes using a combination of exciton-coupled circular dichroism spectroscopy and molecular modeling.[12]

Results

Synthesis of the stilbenosides and oligonucleotide conjugates

The stilbene C-nucleosides α-**St** and β-**St** were prepared as outlined in Schemes 1 and 2, respectively. The key step in Scheme 1 is the cadmium-mediated reaction of the Grignard derivative of *m*-bromostilbene with Hoffer's chlorosugar **10**.[11,13,14] This reaction provides **11** as a 5 : 1 mixture of the α- and β-anomers. The key step in Scheme 2 is coupling of lactone **13** with *m*-bromostilbene, which affords **14** as a 1 : 9 mixture of α- and β-anomers.[14,15] Separation of the anomers and removal of the protecting groups provide the C-nucleosides α-**St** and β-**St**, which are converted to their 5′-dimethoxytrityl (DMT) derivatives **12** and **15** upon reaction with 4,4′-dimethoxytrityl chloride in the presence of diisopropylethylamine. The stable DMT derivatives were converted to their activated derivatives

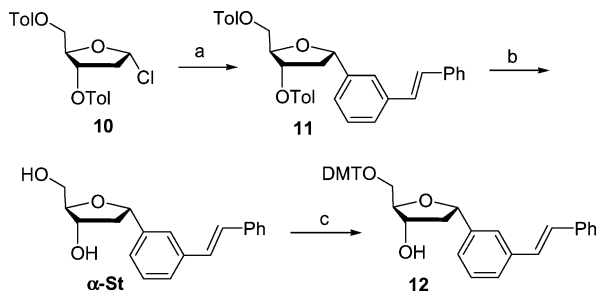

Scheme 1 *Reagents and conditions*: (a) *m*-bromostilbene, Mg, $CdCl_2$, 70%; (b) NaOMe, MeOH, 83%; (c) DMT-Cl, py, DIPEA, 88%.

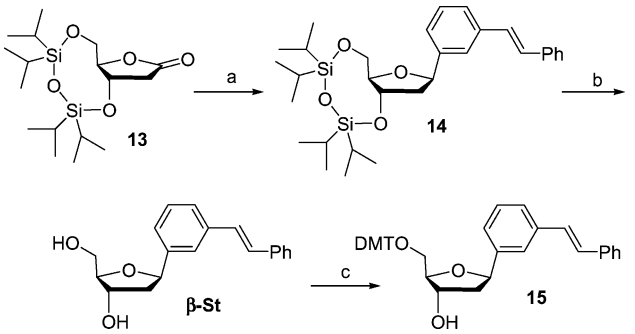

Scheme 2 *Reagents and conditions*: (a) *m*-bromostilbene, n-BuLi, THF −78 °C, 42%; (b) TBAF, THF, 79%; (c) DMT-Cl, py, DIPEA, 88%.

by reaction with 2-cyanoethyl diisopropylchlorophosphoramidite prior to conjugate syntheses. The preparation of *trans*-*N*,*N*′-bis(3-hydroxypropyl)stilbene-4,4′-dicarboxamide (**Sa**) and conversion to its monoprotected, mono-activated diol by sequential reaction with 4,4′-dimethoxytrityl chloride and with 2-cyanoethyl diisopropylchlorophosphoramidite have been described previously.[6]

Oligonucleotide conjugates were prepared by means of conventional phosphoramidite chemistry following the procedure of Letsinger and Wu.[6] Base sequences in which complementary 5′- and 3′-ends are connected either to the base sequence 5′-ACC or to the stilbenedicarboxamide linker **Sa** are known to form stable mini-hairpins.[9,16] The reference hairpins **1**, **4**, and **6** employed in this investigation have short stems consisting of 3 or 5 A:T base-pairs with a single G:C base-pair adjacent to the ACC loops of **1** and **6**. The use of hairpin rather than duplex structures permits study of short, stable base-pair domains. The hairpins are thermodynamically more stable than the corresponding duplexes.[9] A single stilbenoside has been introduced into the hairpin structures as a dangling base (**2**α,β and **5**α,β) and into the interior of the hairpin stem opposite an abasic site (**3**β and **7**α,β). Two stilbenosides have been introduced opposite abasic sites in the interior of the poly(dT) strand of hairpin structure **6**, both in adjacent positions (**8**α,β) and with an intervening dT base (**9**α,β).

UV and fluorescence spectra

The normalized UV absorption spectra of **15**, the DMT derivative of nucleoside β-**St** and the conjugates **2**β and **7**β are shown in Fig. 1. The long-wavelength band is assigned to the allowed π,π* transition of stilbene. This band is slightly red-shifted in the conjugates *vs.* the stilbenoside **15**. The 260 nm band is assigned to the overlapping absorption of the nucleobases and the weaker stilbene absorption. The UV spectral band shapes of conjugates possessing the α- *vs.* β-stilbenosides are indistinguishable, as are the spectra of conjugates possessing two stilbenosides. The 260/315 nm absorbance ratio is proportional to the ratio of the number of base-pairs to stilbenes within the conjugate structure.

Thermal dissociation profiles for the hairpins in Chart 2 were determined at several wavelengths using a Peltier temperature controller to provide a heating rate of 0.5 °C min^{-1}. Hyperchromism is observed for the 260 nm bands of all of the conjugates. Hyperchromism is also observed for the 315 nm bands, in contrast to the hypochromism observed for **Sa**-linked hairpins.[17] First derivatives of the profiles obtained at 260 nm provide melting temperatures which are reported in Table 1. Similar values of

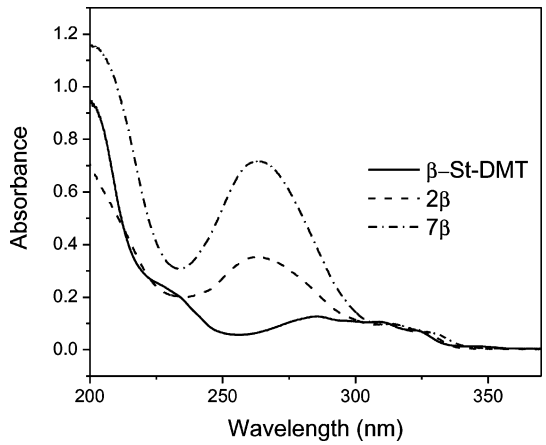

Fig. 1 UV spectra β-**St** (as its mono-DMT derivative **15** in acetonitrile) and conjugates **2**β and **7**β (5 μM in standard buffer).

Table 1 Melting temperature for reference conjugates and conjugates possessing one or two stilbenosides[a]

Hairpin	T_m/°C	ΔT_m/°C
1[b]	36	—
2α	48	12
2β	59	23
3β	33	−3
4[b]	64	—
5α	54 (br)	−10
5β	64	0
6	50	—
7α	47	−3
7β	53	3
8α	46	−4
8β	54	4
9α	46	−4
9β	54	4

[a] Data for 5 μM solutions (0.1 M NaCl, 10 mM phosphate buffer, pH 7.2) obtained with a heating rate of 0.5 °C min^{-1}. [b] Data from ref. 9.

T_m were obtained from 280 nm profiles. In some cases, as noted in Table 1, broad melting transitions and first derivatives were observed.

The fluorescence spectra of the DMT derivative **15** in acetonitrile solution and several conjugates in aqueous buffer are shown in Fig. 2. The vibronic structure observed for **15** is similar to that of *trans*-stilbene, as is its fluorescence quantum yield ($\Phi_f = 0.10$ *vs.* 0.05 for stilbene).[18] The fluorescence of the conjugates is much weaker than that of **15**. In the case of conjugate **3**β, in which the stilbene is located adjacent to a G:C base-pair, a long-wavelength band with a maximum near 450 nm is observed in addition to the quenched monomer band (Fig. 2). The fluorescence intensity for **7**α is approximately twice as large as that of **7**β.

The stilbenoside conjugates are sensitive to ultraviolet light. Continuous 300 nm irradiation of **7**β results in rapid and complete disappearance of its 330 nm absorption band, indicative of loss of stilbene conjugation, rather than *trans*,*cis* photoisomerization. HPLC analysis of the irradiated solutions showed the formation of a complex mixture of products, discouraging attempted product isolation and identification.

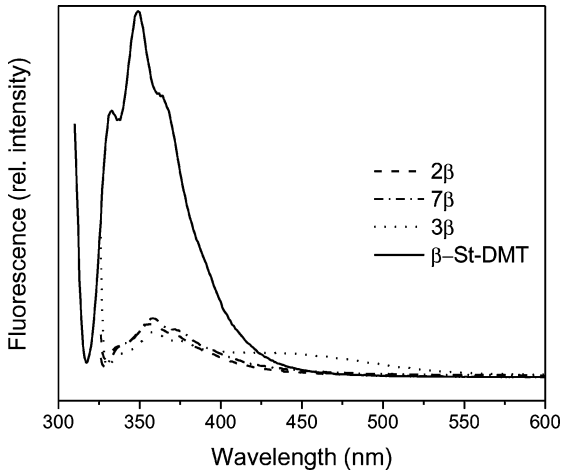

Fig. 2 Fluorescence spectra of β-**St** (as its mono-DMT derivative **15** in acetonitrile) and conjugates **2**β, **3**β, and **7**β (5 μM in standard buffer).

Circular dichroism spectra

The circular dichroism (CD) spectra of conjugates **2**α,β are shown in Fig. 3a. Similar CD spectra were obtained for **3**β and **7**α,β (data not shown). The bands in the 200–300 nm spectral region are attributed to exciton coupling between the adjacent base-pairs, and are similar to those of the mini-hairpins **1** and **6**.[19] Weak negative bands are observed in the 300–340 nm spectral region of **2**α,β. The CD spectra of conjugates **5**α,β, **8**α,β, and **9**α,β are shown in Fig. 3b,c. Their spectra in the base-pair region (200–300 nm) are similar to those of the mini-hairpins **1** and **6**. In addition, they

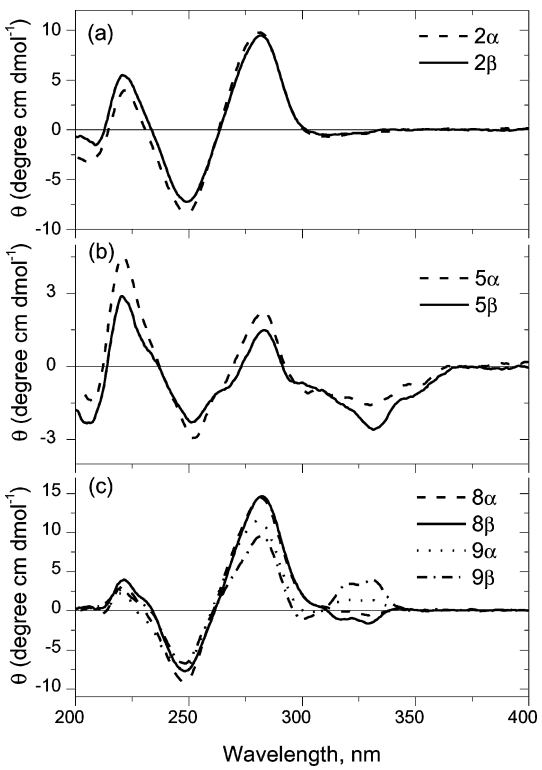

Fig. 3 CD spectra of (a) conjugates **2**α and **2**β, (b) conjugates **5**α and **5**β (matched absorbance at 327.5 nm), and (c) conjugates **8**α, **8**β, **9**α, and **9**β (matched absorbance at 316 nm) all in standard buffer.

This journal is © The Royal Society of Chemistry 2006

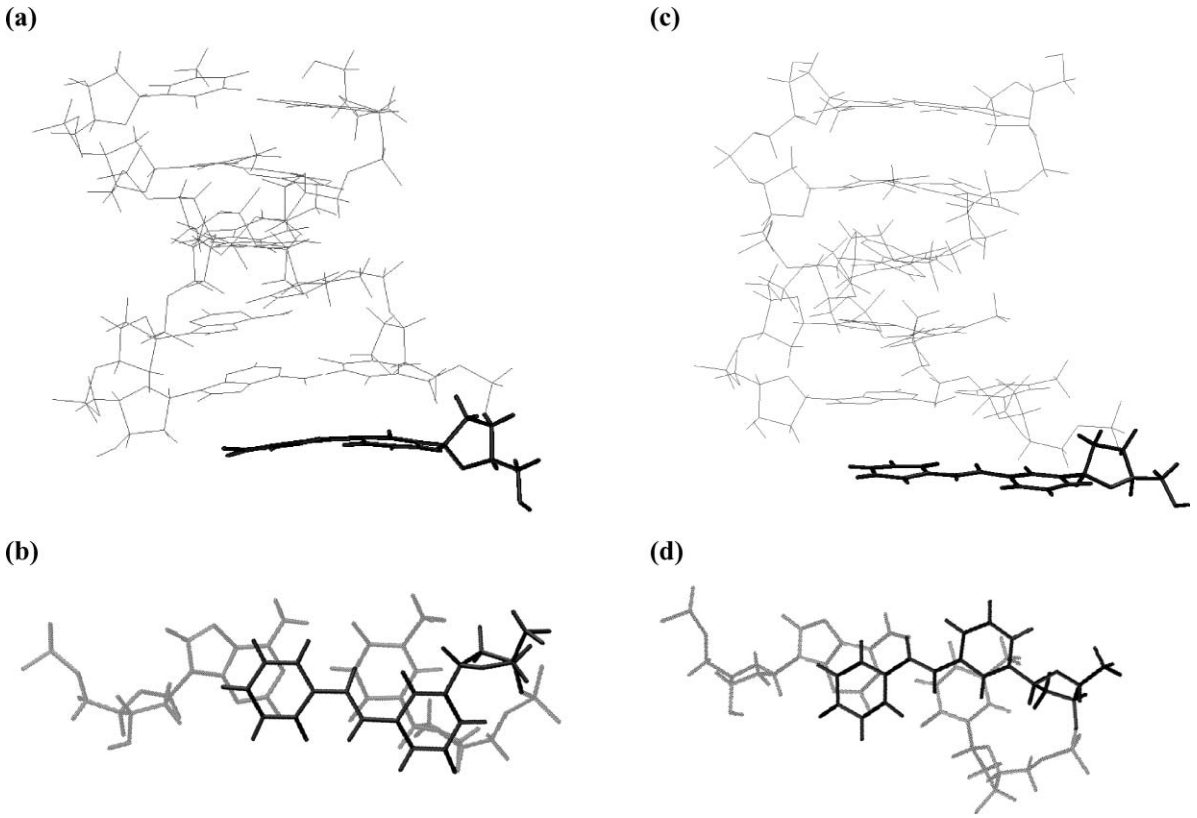

Fig. 4 Perspective view of the structures obtained from molecular dynamics simulations (loop regions omitted) viewed from the side and from the stilbene end for **2**α (a and b) and **2**β (c and d). Stilbenosides are bold. The twist angles between the stilbene and base-pair long axes are $-9 \pm 16°$ for **2**α and $38 \pm 6°$ for **2**β.

have bands in the 300–350 nm spectral region which are more intense than those of **2**α,β and differ in both sign and intensity.

Molecular dynamics simulations

Geometries for the DNA duplex domains of **2**α,β, **7**α,β, **8**α,β, and **9**α,β calculated using the AMBER force field by adopting the canonical A_6T_6 B-form DNA structure for their base-pair domains.[20] Similar methods as described in previous work were used to calculated the charge parameters of the stilbenoside residues and to equilibrate the simulation systems.[9] The Amber 7.0 program suite was used to run molecular dynamics simulations in the explicit water solution.[21] The total simulation time for each conjugate structure was 4.0 ns with a time step length of 2 fs. The resulting structures represent local minima arrived at from idealized B-DNA input structures. The twist angle and distance between stilbenes and neighboring DNA base-pairs were calculated by fitting the trajectories using Curves 5.2.[22]

Averaged structures obtained from multiple MD snapshots for **2**α,β are shown in Fig. 4. In both structures, the stilbene is approximately parallel to the adjacent base-pairs with π-stacking distances of 3.2 ± 0.8 Å and 3.4 ± 0.4 Å for **2**α and **2**β, respectively. The calculated structure for **2**β has a normal helical pitch of $38 \pm 6°$ between the long axes of stilbene and the adjacent base-pair. However, the twist angle for **2**α is $-9 \pm 16°$, a negative twist being necessary to provide an extent of π-stacking similar to that for **2**β.

Averaged structures for **7**α,β are shown in Fig. 5. Both structures display significant perturbation of B-DNA geometry. This is most pronounced for **7**α, in which the stilbene is extrahelical. The stilbene in **7**β has a smaller base-stacking distance (3.4 ± 0.4 Å *vs.* 4.2 ± 0.4 Å) and also a smaller twist angle ($11 \pm 5°$ *vs.* $56 \pm 6°$) in the 3′T *vs.* 5′T direction. As is the case for **7**α and **7**β, the calculated structures for **8**α and **9**α have extrahelical stilbenes (structures not shown), whereas the calculated structures for **8**β and **9**β have intrahelical stilbenes (see ESI†). The dihedral angles between stilbenes in **8**α and **8**β are relatively small ($-18 \pm 13°$ and $1 \pm 8°$, respectively), when compared to the dihedral angles between stilbenes in **9**α and **9**β ($77 \pm 10°$ and $52 \pm 8°$, respectively). The rise and helical pitch for **8**β and **9**β are larger in the 5′- *vs.* 3′-direction, as is the case for **7**β. The π-stacking distance between stilbenes in **8**β is 3.8 ± 0.5 Å.

Discussion

Capping stilbenosides

The addition of a stilbenoside to the mini-hairpin **1** as a dangling base results in a marked increase in hairpin stability for both **2**α and **2**β. The increase in T_m for **2**β is approximately twice as large as that for **2**α (Table 1). Similarly, the value of T_m for **5**β is the same as that for the capped hairpin **4**, which has a singly tethered **Sa** end-cap, whereas the T_m for **5**α is 10° lower. Increased thermodynamic stability has previously been observed for hairpin structures possessing hydrophobic stilbene capping groups.[8–10] The value of ΔT_m for a derivative of **1** possessing a **Sa**

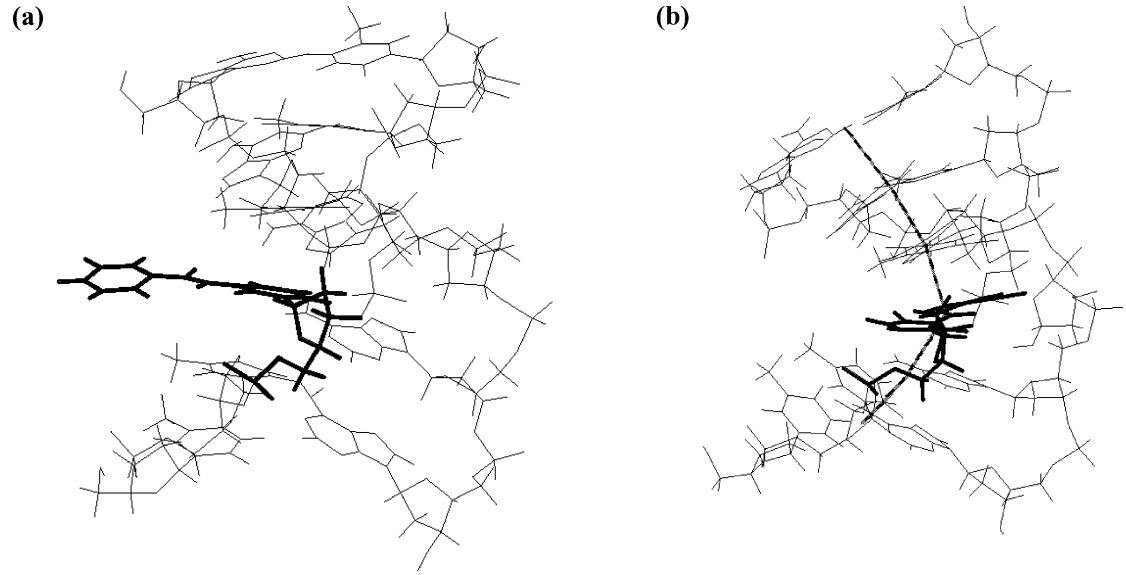

Fig. 5 Averaged truncated structures (loop regions omitted) for (a) **7**α and (b) **7**β (dashed line shows center of base-pairs) obtained from molecular dynamics simulations. Stilbenosides are bold.

linker attached to the 5′-terminus of **1** *via* a flexible linker is 18 °C, intermediate between the values for **2**α and **2**β.[8,9] The presence of an **Sa** capping group in hairpin **4** also results in a significant increase in T_m. Kool and co-workers have investigated the thermodynamics of melting for self-complementary duplexes having a dangling synthetic β-nucleosides possessing aromatic hydrocarbon hydrophobic groups, the most effective of which is β-**Py** (Chart 1, $\Delta T_m = 23.1$ °C for 5 μM duplex in 1.0 M NaCl).[3] Dogan *et al.* report a similar value of ΔT_m for a self-complementary duplex with a 5′-tethered stilbene.[10] Both the pyrenoside and the tethered stilbene duplexes have two hydrophobic aromatic capping groups, whereas **2**β has a single capping group. Thus the unsubstituted stilbene ring of **2**β appears to have a hydrophobic capping effect on duplex stability comparable to or greater than those of Kool's β-**Py** or Dogan's stilbene.

The CD spectra of **2**α,β and **5**α,β in the base-pair region (200–300 nm, Fig. 3a,b) are similar to those of **1** and **4**, and presumably are dominated by the short A_3:T_3 base-pair domains (A-tracts). Molecular modeling (Fig. 4) suggests that **2**β adopts a more "normal" B-DNA capping geometry with a rise of 3.4 Å and a helical pitch of 38° between the stilbene long axis and the adjacent A:T base-pair. In comparison, **2**α adopts a smaller helical pitch of −9°, presumably in order to achieve optimal stilbene–base-pair overlap.

Internal stilbenosides

The presence of a stilbenoside opposite an abasic site in the interior of the base-pair stem of the mini-hairpin **3**β results in a small decrease in thermal stability when compared to **1** (Table 1). Comparison of the T_m values for **7**α,β with those for **6** indicates that **7**β is slightly more stable and **7**α is slightly less stable. Kool and co-workers observed a similar increase in T_m for duplexes possessing β-**Py** opposite an abasic site.[4,5] The CD spectra of **3**β and **7**α,β in the base-pair region is similar to those of **1** or **6**, and presumably is dominated by the short A-tracts.

The effect of an abasic site on the structure and stability of duplex DNA has been extensively investigated.[23,24] Duplexes in which a purine nucleobase is located opposite the abasic site are generally more stable than those with a pyrimidine opposite the abasic site; however both apurinic and apyrimidinic duplexes adopt B-DNA geometries with intrahelical bases.[24] The presence of a single α-dA nucleoside opposite dT in a 9-mer duplex causes only a small decrease in duplex stability ($\Delta\Delta G^\circ = 0.2$ kcal mol^{-1}) when compared to a normal β-dA–dT base-pair.[25] Molecular modeling indicates that the α-dA–dT base-pair has an intrahelical base-paired structure. The inability of the α-**St**–**X** base-pair to form a hydrogen-bonded structure may account for the extrahelical location of the stilbene in **7**α predicted by molecular modeling (Fig. 5a). In the case of **7**β, the increase in base-stacking of the intrahelical stilbene may be limited by the poor overlap with the base-pair in the 5′T direction, as predicted by molecular modeling (Fig. 5b).

Two internal stilbenosides

Incorporation of a second stilbenoside into the hairpin structure **6** causes little additional change in the T_m values of **8**α,β or **9**α,β when compared to **7**α,β (Table 1). Their base-pair CD spectra (Fig. 3c) are similar to those of **2**α,β (Fig. 3a), indicating that the short A-tract base-pair domains separating the hairpin loop and proximal stilbene remain largely intact. Matray and Kool prepared a duplex having two β-**Py**–**X** base-pairs separated by two intervening G:C base-pairs.[4] They report an abnormal thermal dissociation profile with a high apparent T_m, but a CD spectrum characteristic of B-DNA.

The calculated structures of **8**α and **9**α (not shown) are highly disordered with extrahelical stilbenes. The calculated structures of **8**β and **9**β both have intrahelical stilbenes with distorted base-paired geometries in the region of the two stilbenosides (see ESI†). The two stilbenes in **8**β have a slipped parallel relationship in which the stilbene long axes are aligned with a π-stacking

 This journal is © The Royal Society of Chemistry 2006

distance of 3.8 ± 0.5 Å. The slipped geometry reduces electron–electron repulsion and is commonly observed for pairs of aromatic molecules.[26] The two stilbenes in **9**β have a parallel geometry with a dihedral angle of 52 ± 8°, somewhat smaller than the value for two 36° steps in B-DNA. The calculated stilbene–stilbene dihedral angles are consistent with the EC-CD spectra (*vide infra*). However, it should be borne in mind that the calculated structures represent local minima and may not accurately reflect the solution structure of these conjugates.

Electronic interactions

Small red-shifts are observed in the long wavelength region of the absorption spectra for conjugates **2**α,β, **3**β, and **7**α,β when compared to the spectra of the mono-DMT derivative of β-**St** (Fig. 1). We have attributed similar UV spectral shifts for **Sa**-linked hairpins and capped hairpins to weak electronic interactions between the stilbene chromophore and adjacent base-pair.[8,9,17] The weak long-wavelength CD bands for **2**α,β (Fig. 3a), **3**β, and **7**α,β are also similar to those observed for **Sa**-linked hairpins and capped hairpins. These bands are attributed to induced circular dichroism, by analogy to the CD spectra of intercalating dyes which have their long axes parallel to those of the adjacent base-pairs.[27]

Efficient quenching of stilbene fluorescence in **2**α,β, **3**β, and **7**α,β by neighboring nucleobases (Fig. 2) prevents the use of the stilbenosides as intrinsic fluorescence probes of the base-pair dynamics. Quenching might occur *via* either electron transfer or a photochemical reaction involving the stilbene and a neighboring base. Quenching of the fluorescence of stilbene hairpin linkers having either electron-accepting or electron-donating substituents by neighboring base-pairs has been attributed to electron transfer in which the excited stilbene singlet can served as either an electron acceptor or donor.[7,17] An alternative explanation for the efficient fluorescence quenching of the stilbenoside conjugates is the occurrence of photochemical addition reactions between the stilbene and adjacent nucleobases. Both stilbene and thymine are known to undergo efficient [2 + 2] duplex-templated photodimerization reactions.[28] Stilbene photodimerization is possible for **8**α,β, but not for the other conjugates. Cross-addition between stilbene and thymine could account for the occurrence of efficient fluorescence quenching, bleaching of the stilbene 315 nm absorption band, and the complex appearance of HPLC traces for irradiated solutions.

Conjugates **5**α,β, **8**α,β, and **9**α,β, which possess two stilbene chromophores, have stronger long-wavelength CD bands than do conjugates possessing a single stilbene chromophore (Fig. 3). These CD bands are attributed to exciton coupling (EC-CD) between the two stilbene chromophores.[29,30] As previously reported for capped hairpin structures possessing two **Sa** chromophores, exciton coupling results in the observation of bisignate CD spectra, the sign and intensity of which are dependent upon both the distance between the stilbene chromophores and the dihedral angle between their electronic transition dipoles.[8,9] A second, shorter wavelength band of the EC-CD spectrum should appear below 300 nm but is largely obscured by the strong positive 280 nm band of the base-pair CD spectrum.

The intensity of the positive and negative bands of the EC-CD spectrum for two identical parallel chromophores can be described by eqn (1),

$$\Delta\varepsilon \approx \pm\frac{\pi}{4\lambda}\mu_a\mu_d R_{da}^{-2}\sin(2\theta) \quad (1)$$

where μ_d and μ_a are the electronic transition dipole moments of the two chromophores, R_{da} is their center-to-center distance, and θ is the angle between their transition dipoles.[8,9,29,31] The $\sin(2\theta)$ dependence results in zero intensity when $\theta = 0$, 90, or 180°, and maximum intensity when $\theta = 45$ or 135°. The low EC-CD intensity for **8**β (Fig. 3c) is consistent with the small dihedral angle between the stilbene long-axes obtained from molecular modeling (1 ± 8°). Significantly higher intensity EC-CD bands are observed for **9**β (Fig. 3c) even though the value of R_{da} is approximately twice as large as that for **8**β. The larger EC-CD intensity is consistent with the calculated dihedral angle (52 ± 8°) which is close to the optimum angle of 45°. The weaker EC-CD signals for the α-stilbenosides **8**α and **9**α may reflect their highly disordered, fluctional structures. We note that the intensity of the EC-CD spectrum is dependent upon the magnitude of the transition dipoles as well as the geometry of the two coupled chromophores. The larger dipole for the stilbene *vs.* pyrene long-wavelength transition makes the stilbenosides better suited for this application.

The CD spectra of conjugates **5**α and **5**β (Fig. 3b) display moderately intense negative bands in the 300–350 nm spectral region attributed to exciton coupling between the **Sa** and **St** chromophores. The irregular band shapes are a consequence of coupling between chromophores with different absorption maxima.[31] The EC-CD intensity for **5**β is stronger than that for **5**α, indicative of a difference in capping structure similar to that calculated for **2**α *vs.* **2**β (Fig. 4). The **Sa**-capped hairpin **4** (Chart 2), which has three intervening A:T base-pairs also has a negative long-wavelength EC-CD band.[9]

Concluding remarks

The structure and properties of oligonucleotides possessing synthetic stilbene C-nucleosides have been investigated for the first time. Both the α- and β-stilbenosides stabilize duplex structures when employed as dangling end-capping groups in conjugates **2**α,β and **5**α,β. When incorporated into duplex interior opposite an abasic site, the β-anomer results in a modest increase in duplex stability, whereas the presence of the α-anomer destabilizes the duplex. Similar results were obtained for conjugates possessing two stilbenosides either adjacent to each other or separated by one base-pair. The ability of the β-stilbenoside to stabilize duplex structures either as a capping group or opposite an abasic site within the duplex interior is similar to that of Kool's β-pyrenoside.

Molecular modeling indicates that the difference in stability of duplexes possessing α- *vs.* β-stilbenosides can be related to their structures. As capping groups, both anomers adopt structures in which the stilbene effectively covers the hydrophobic face of the terminal base-pair. However, when located within the base-pair domain, the α-anomer adopts an extrahelical geometry whereas the β-anomer adopts an intrahelical geometry. The strong electronic transition dipole moment of the stilbene chromophore permits observation of exciton-coupled circular dichroism for conjugates possessing two stilbene chromophores. The combination of EC-CD spectroscopy with molecular modeling permits assignment of the relative geometry of the two chromophores.

Experimental

Synthetic procedures

All reactions were carried out under an argon atmosphere with dry solvents under anhydrous conditions, unless otherwise noted. Yields refer to chromatographically and spectroscopically (^{1}H NMR) homogeneous materials, unless otherwise stated. Reagents purchased were of the highest commercial quality and used without further purification, unless otherwise stated. Methylene chloride and chloroform were distilled from calcium hydride. Tetrahydrofuran (THF) was distilled from sodium/benzophenone. Methanol was distilled from magnesium. Analytical thin-layer chromatography (TLC) was performed using 0.25 mm pre-coated silica gel Kieselgel 60 F_{254} plates. Visualization of the chromatogram was by UV absorbance, iodine, dinitrophenylhydrazine, ceric ammonium molybdate, ninhydrin or potassium permanganate, as appropriate. Preparative and semi-preparative TLC was performed using Merck 1 mm or 0.5 mm coated silica gel Kieselgel 60 F_{254} plates respectively. Merck silica gel (60, particle size 0.040–0.063 mm) was used for flash column chromatography. NMR spectra were recorded on a Varian 300 MHz instrument and calibrated using residual undeuterated solvent as an internal reference. The following abbreviations were used to explain the multiplicities: s = singlet, d = doublet, ddd = doublet of doublets, t = triplet, m = multiplet. Electrospray ionization (ESI) time-of-flight reflectron experiments were performed on an Agilent ESI-TOF mass spectrometer. Samples are electrosprayed into the TOF reflectron analyzer at an ESI voltage of 4000 V and a flow rate of 200 μL min^{-1}). Compounds **10**,[13] **13**,[15] and 3-bromostilbene[32] were synthesized according to literature procedures.

1,2-Dideoxy-α-1-[3-*trans*-stilbene]-3,5-di-*O*-(*p*-toluoyl)-D-erythro-pentitol (11). A solution of *m*-bromostilbene[32] (700 mg, 2.70 mmol) in THF (15 mL) was slowly added to Mg turnings (139 mg, 3.38 mmol). After the addition of ~2 mL of the *m*-bromostilbene solution, I_2 crystals and two drops of dibromoethane were added to start the reaction. The rest of the *m*-bromostilbene was then added slowly, and the solution heated under reflux for 2 h. Subsequently, $CdCl_2$ (576 mg, 3.14 mmol) was added, and the mixture was heated for another 2 h under reflux. After cooling to room temperature, a solution of chlorosugar **10**[13] (1.22 g, 3.14 mmol) was added slowly *via* a dropping funnel and stirred for 16 h. The solution was dried *in vacuo* to remove the THF and the residue was dissolved in CH_2Cl_2. The resulting organic solution was washed twice with saturated NH_4Cl and dried over Na_2SO_4. The mixture was concentrated *in vacuo* and purified by flash chromatography (EtOAc–hexanes, from 1 : 7 to 1 : 5) to yield the desired compound as a white foam (1.0 g, 70% yield). α : β 5 : 1. ^{1}H NMR ($CDCl_3$, 300 MHz) δ 7.56–7.51 (m, 3H), 7.48–7.42 (m, 3H), 7.38–7.16 (m, 13H), 7.13 (s, 2H), 6.85 (d, 4H, J = 8.8 Hz), 5.16 (dd, 1H, J = 7.4 Hz), 4.46 (m, 1H), 4.22 (ddd, 1H, J = 6.0, 4.6, 4.6), 3.80 (s, 6H), 3.41 (dd, 1H, J = 9.4, 4.6 Hz), 3.25 (dd, 1H, J = 9.4, 6.0 Hz), 2.73 (m, 1H), 2.07 (m, 1H). ^{13}C{^{1}H} NMR ($CDCl_3$, 75 MHz) δ 166.4, 166.1, 144.0, 143.8, 142.9, 137.5, 137.2, 129.8, 129.7, 129.6, 129.1, 129.1, 129.1, 128.9, 128.7, 128.7, 128.6, 128.5, 127.6, 127.0, 126.8, 126.5, 125.6, 125.0, 123.7, 82.4, 80.2, 64.6, 40.2, 21.7. ESI-TOF calc. $C_{35}H_{32}O_5$ [M + H$^+$]: 533.2322, found: 533.2313.

1,2-Dideoxy-α-1-(3-*trans*-stilbene)-D-ribofuranose (α-St). Freshly prepared 0.5 M NaOMe in MeOH was added to a solution of protected nucleoside **11** (500 mg, 0.835 mmol) in 1 : 1 MeOH–CH_2Cl_2 (10 mL). After stirring for 4 h at room temperature, saturated NH_4Cl (20 mL) was added, and the solvent was evaporated. The crude material was purified using flash chromatography (CH_2Cl_2–MeOH, 19 : 1) to yield the desired compound as a white solid (205 mg, 83% yield). ^{1}H NMR ($CDCl_3$, 300 MHz) δ 7.46–7.16 (m, 9H), 7.05 (s, 2H), 5.05 (dd, 1H, J = 7.3 Hz), 4.40 (dd, 1H, J = 6.5, 6.5 Hz), 4.07–4.04 (m, 1H), 3.72 (m, 2H), 2.63 (ddd, 1H, J = 13.2, 6.5, 6.5 Hz), 2.07–2.01 (m, 1H). ^{13}C{^{1}H} NMR ($CDCl_3$, 75 MHz) δ 142.9, 137.9, 137.4, 129.3, 129.1, 128.9, 128.6, 127.9, 126.7, 126.1, 125.1, 123.9, 85.4, 79.8, 73.2, 62.6, 43.6. ESI-TOF calc. $C_{19}H_{20}O_3$ [M + Na$^+$]: 319.1305, found: 319.1305.

1,2-Dideoxy-α-1-(3-*trans*-stilbene)-5-*O*-*p*-dimethoxytrityl-D-ribofuranose (12). The C-nucleoside **β-St** (430 mg, 1.45 mmol) was dissolved in a 1 : 1 mixture of pyridine and methylene chloride (18 mL). Diisopropylethylamine (280 mg, 2.17 mmol) and 4,4′-dimethoxytrityl (DMT) chloride (982 mg, 2.90 mmol) were added to the mixture and stirred for 4 h at room temperature and then quenched with methanol (10 mL). The resulting mixture was concentrated *in vacuo* and purified by flash chromatography (EtOAc–hexanes, from 1 : 5 to 1 : 1) to yield the desired compound as a yellow foam (764 mg, 88% yield). ^{1}H NMR (C_6D_6, 300 MHz) δ 7.69–7.65 (m, 3H), 7.51 (dd, 4H, J = 9.1, 1.8 Hz), 7.29–6.97 (m, 12H), 6.73 (d, 4H, J = 9.1 Hz), 5.05 (dd, 1H, J = 7.3, 7.3 Hz), 4.31 (ddd, 1H, J = 5.0, 5.0, 5.0 Hz), 4.23 (ddd, 1H, J = 5.0, 5.0, 5.0 Hz), 3.54 (dddd, 2H, J = 5.0, 5.0, 5.0, 5.0 Hz) 3.25 (s, 3H), 2.24 (s, 1H), (dd, 1H, J = 12.6, 6.8, 6.8 Hz), 1.87 (ddd, 1H, J = 12.6, 6.8, 6.8 Hz). ^{13}C{^{1}H} NMR (C_6D_6, 75 MHz) δ 159.0, 145.7, 144.3, 137.7, 137.7, 136.4, 136.5, 129.1, 129.0, 128.8, 128.7, 128.6, 128.0, 127.6, 126.9, 126.8, 125.6, 125.3, 124.3, 86.6, 85.2, 79.7, 74.7, 65.1, 54.6, 43.9. ESI-TOF calc. $C_{40}H_{38}O_5$ [M + Na$^+$]: 621.2611 found: 621.2612.

3,5-*O*-((1,1,3,3-Tetraisopropyl)disiloxanediyl)-1,2-dideoxy-β-1-(3-*trans*-stilbene)-D-ribofuranoses (14). To a solution of the 3-bromo-*trans*-stilbene[32] (2.1 g, 8.32 mmol) in anhydrous THF (20 mL) under N_2 and at −78 °C was added n-BuLi (5.2 mL of 1.8 M in hexanes). The mixture was stirred at −78 °C for 30 min and was then added *via* cannula to a solution of **13**[15] (2.0 g, 5.34 mmol) in anhydrous THF (20 mL) at −78 °C. After 1 h, the reaction mixture was quenched at −78 °C with sat. aqueous NH_4Cl (80 mL) and then extracted with diethyl ether (2 × 200 mL). The combined ether phases were washed with sat. aqueous NH_4Cl, water, and brine, and were dried over anhydrous Na_2SO_4. Concentration *in vacuo* produced an oil that was used without further purification. A solution of the crude oil in CH_2Cl_2 (20 mL) under N_2 and at −78 °C was treated with Et_3SiH (1.86 g, 16.00 mmol) and $BF_3{\cdot}OEt_2$ (2.27 g, 16.00 mmol). The resulting solution was stirred at −78 °C for 6 h, and then quenched at −78 °C by the addition of sat. $NaHCO_3$ (100 mL). The resulting mixture was extracted with CH_2Cl_2 (2 × 50 mL). The combined organic phases were dried over anhydrous Na_2SO_4 and concentrated *in vacuo*. Flash chromatography of the crude product using toluene as the eluent yielded the desired compound as a colorless oil (1.2 g, 42% yield) α : β 1 : 9. ^{1}H NMR ($CDCl_3$, 300 Hz) δ 7.52–7.46 (m, 4H), 7.42–7.21 (m, 8H), 7.09 (s, 2H), 5.10 (dd, 1H, J = 7.2,

 This journal is © The Royal Society of Chemistry 2006

7.2 Hz), 4.53 (m, 1H), 4.15 (m, 1H), 3.91 (m, 2H), 2.38 (ddd, 1H, J = 12.7, 6.8, 4.3), 2.09 (ddd, 1H, J = 12.7, 6.8, 6.8 Hz), 2.13–0.93 (m, 24H). $^{13}C\{^1H\}$ NMR ($CDCl_3$, 300 Hz) δ 139.1, 135.2, 135.1, 128.8, 128.7, 128.5, 128.0, 127.8, 127.7, 127.7, 126.5, 126.4, 125.8, 123.5, 94.2, 82.3, 70.7, 62.9, 13.2, 12.5. ESI-TOF calc. $C_{31}H_{46}O_4Si_2$ [M + H^+]: 538.2935, found: 538.2933.

1,2-Dideoxy-β-1-(3-*trans*-stilbene)-D-ribofuranose (β-St). To a solution of **14** (1.2 g, 2.22 mmol) in THF (44 mL) was added tetrabutylammonium fluoride (6.66 mL of 1 M solution in THF). The resulting mixture was stirred at room temperature for 3 h, then 5% aqueous NH_4HCO_3 (100 mL) was added to quench the reaction. The mixture was extracted with diethyl ether (3 × 100 mL), and the combined organic extracts were washed with 5% aqueous NH_4HCO_3 (100 mL), water (100 mL), and brine (100 mL). The organic layer was then dried over anhydrous Na_2SO_4 and concentrated *in vacuo* to give the crude product as a white solid. The crude material was purified using flash chromatography (CH_2Cl_2–MeOH, 19 : 1) to yield the desired compound as a white solid (520 mg, 79% yield). ^1H NMR ($CDCl_3$, 300 MHz) δ 7.44–7.13 (m, 9H), 5.11 (dd, 1H, J = 10.3, 5.9 Hz), 4.36–4.34 (m, 1H), 3.99–3.95 (m, 1H), 3.79–3.67 (m, 2H), 2.22 (ddd, 1H, J = 13.2, 5.6, 1.5 Hz), 1.97 (m, 1H). $^{13}C\{^1H\}$ NMR ($CDCl_3$, 75 MHz) 141.6, 137.8, 137.3, 129.3, 129.1, 128.9, 128.5, 127.9, 126.7, 126.1, 125.4, 125.4, 87.3, 80.3, 73.9, 63.5, 43.9. ESI-TOF calc. $C_{19}H_{20}O_3$ [M + Na^+]: 319.1305, found: 319.1306.

1,2-Dideoxy-β-1-(3-*trans*-stilbene)-5-*O*-*p*-dimethoxytrityl-D-ribofuranose (15). The C-nucleoside **β-St** (430 mg, 1.45 mmol) was dissolved in a 1 : 1 mixture of pyridine and methylene chloride (18 mL). Diisopropylethylamine (280 mg, 2.17 mmol) and 4,4′-dimethoxytrityl (DMT) chloride (982 mg, 2.90 mmol) were added to the mixture and the reaction was stirred for 4 h at room temperature and then quenched with methanol (10 mL). The resulting mixture was concentrated *in vacuo* and purified by flash chromatography (EtOAc–hexanes, from 1 : 5 to 1 : 1) to yield the desired compound as a yellow foam (764 mg, 88% yield). ^1H NMR (C_6D_6, 300 MHz) δ 7.84 (s, 1H), 7.70 (d, 2H, J = 7.3 Hz), 7.53 (dd, 4H, J = 8.8, 3.0 Hz), 7.29–7.22 (m, 3H), 7.18–6.96 (m, 12H), 6.72 (d, 4H, J = 8.8 Hz), 5.26 (dd, 1H, J = 8.5, 8.5 Hz), 4.15 (t, 2H, J = 3.5 Hz), 3.54 (dd, 1H, J = 9.7, 4.1 Hz), 3.39 (dd, 1H, J = 9.7, 4.1 Hz), 3.21 (s, 3H), 3.20 (s, 3H), 2.04–2.00 (m, 2H). $^{13}C\{^1H\}$ NMR (C_6D_6, 75 MHz) δ 159.0, 145.8, 143.4, 137.9, 137.6, 136.5, 130.5, 130.5, 129.2, 128.9, 128.8, 128.7, 128.1, 127.0, 126.8, 126.1, 125.8, 124.5, 87.1, 86.6, 80.3, 74.6, 65.1, 54.6, 44.8. ESI-TOF calc. $C_{40}H_{38}O_5$ [M + Na^+]: 621.2611, found: 621.2610.

Synthesis of oligonucleotide conjugates

The preparation of *trans*-*N*,*N*′-bis(3-hydroxypropyl)stilbene-4,4′-dicarboxamide (**Sa**) and conversion to its monoprotected, monoactivated diol by sequential reaction with 4,4′-dimethoxytrityl chloride and with 2-cyanoethyl diisopropylchlorophosphoramidite followed literature procedures.[6] Oligonucleotide conjugates were synthesized by means of conventional phosphoramidite chemistry using a Millipore Expedite DNA synthesizer following the procedure of Letsinger and Wu.[6] All other reagents, including abasic nucleotide, 2′-deoxynucleotide phosphoramidites, DNA-synthesizing reagents, and controlled-pore glass solid supports (CPG) were purchased from Glen Research (Sterling, VA). Following synthesis, the conjugates were first isolated as trityl-on derivatives by reverse phase (RP) HPLC, then detritylated in 80% acetic acid for 30 min, and repurified by RP-HPLC as needed. RP-HPLC analysis was carried out on a chromatograph with a Phenomenex Hyperclone ODS-5 (C18) column (4.6 × 250 mm) and a 1% gradient of acetonitrile in 0.03 M triethylammonium acetate buffer (pH 7.0) with a flow rate of 1.0 mL min^{-1}. Molecular weights were determined by means of MALDI TOF mass spectroscopy following desalting using a NAP 5 column.

Electronic spectroscopy

UV spectra and thermal dissociation profiles were determined using a Perkin–Elmer lambda 2 UV spectrophotometer equipped with a Peltier temperature programmer for automatically increasing the temperature at the rate of 0.5 °C min^{-1}. Circular dichroism spectra were obtained using a JASCO J-715 spectrometer at the indicated concentrations. Fluorescence studies were obtained using a Spex FluoroMax spectrometer. Photo-irradiation was carried out in a Rayonet reactor equipped with 300 nm lamps. Unless otherwise noted, all the spectroscopic studies were done in 0.1 M NaCl, 10 mM Phosphate buffer (pH 7.2, standard buffer) using freshly prepared sample solutions.

Acknowledgements

Financial support for this research was provided by grants from the National Science Foundation (CHE-0400663 to FDL) and The Skaggs Institute for Chemical Biology (KDJ).

References

1 V. A. Bloomfield, D. M. Crothers and I. Tinoco, Jr., *Nucleic Acids: Structures, Properties, Functions*, University Science Books, Sausalito, CA, 2000; S. Neidle, *Oxford Handbook of Nucleic Acid Structure*, Oxford University Press, Oxford, 1999.
2 E. T. Kool, *Acc. Chem. Res.*, 2002, **35**, 936–943.
3 K. M. Guckian, B. A. Schweitzer, R. X.-F. Ren, C. J. Sheils, P. L. Paris and E. T. Kool, *J. Am. Chem. Soc.*, 1996, **118**, 8182–8183; K. M. Guckian, B. A. Schweitzer, R. X.-F. Ren, C. J. Sheils, D. C. Tahmassebi and E. T. Kool, *J. Am. Chem. Soc.*, 2000, **122**, 2213–2222.
4 T. J. Matray and E. T. Kool, *J. Am. Chem. Soc.*, 1998, **120**, 6191–6192.
5 S. Smirnov, T. J. Matray, E. T. Kool and C. de los Santos, *Nucleic Acids Res.*, 2002, **30**, 5561–5569.
6 R. L. Letsinger and T. Wu, *J. Am. Chem. Soc.*, 1995, **117**, 7323–7328.
7 F. D. Lewis, Y. Wu and X. Liu, *J. Am. Chem. Soc.*, 2002, **124**, 12165–12173.
8 F. D. Lewis, X. Liu, Y. Wu and X. Zuo, *J. Am. Chem. Soc.*, 2003, **125**, 12729–12731.
9 F. D. Lewis, L. Zhang, X. Liu, X. Zuo, D. M. Tiede, H. Long and G. C. Schatz, *J. Am. Chem. Soc.*, 2005, **127**, 14445–14453.
10 Z. Dogan, R. Paulini, J. A. Rojas Stutz, S. Narayanan and C. Richert, *J. Am. Chem. Soc.*, 2004, **126**, 4762–4763.
11 C. Strässler, N. E. Davis and E. T. Kool, *Helv. Chim. Acta*, 1999, **82**, 2160–2171.
12 Y. Zheng, H. Long, G. C. Schatz and F. D. Lewis, *Chem. Commun.*, 2005, 4795–4797.
13 N. C. Chaudhuri and E. T. Kool, *Tetrahedron Lett.*, 1995, 1795–1798.
14 D.-W. Chen, A. E. Beuscher, IV, R. C. Stevens, P. Wirsching, R. A. Lerner and K. D. Janda, *J. Org. Chem.*, 2001, **66**, 1725–1732.
15 U. Wichai and S. A. Woski, *Org. Lett.*, 1999, **1**, 1173–1175.
16 S. Yoshizawa, G. Kawai, K. Watanabe, K. Miura and I. Hirao, *Biochemistry*, 1997, **36**, 4761–4767.
17 F. D. Lewis, T. Wu, X. Liu, R. L. Letsinger, S. R. Greenfield, S. E. Miller and M. R. Wasielewski, *J. Am. Chem. Soc.*, 2000, **122**, 2889–2902.

18 J. Saltiel and Y.-P. Sun, in *Photochromism: Molecules and Systems*, ed. H. Durr and H. Bouas-Laurent, Elsevier, Amsterdam, 1990.
19 W. C. Johnson, in *Circular Dichroism: Principles and Applications*, ed. N. Berova, K. Nakanishi and R. W. Woody, Wiley-VCH, New York, 2000, pp. 741–768.
20 W. D. Cornell, P. Cieplak, C. I. Bayly, I. R. Gould, K. M. Merz, D. M. Ferguson, D. C. Spellmeyer, T. Fox, J. W. Caldwell and P. A. Kollman, *J. Am. Chem. Soc.*, 1996, **118**, 2309–2309; S. Arnott, P. J. Campbell-Smith and R. Chandrasekaran, in *Handbook of Biochemistry and Molecular Biology* (3rd edn), CRC Press, Cleveland, OH, 1976, pp.411–422.
21 AMBER 7, 2002.
22 R. Lavery and H. Sklenar, *J. Biomol. Struct. Dyn.*, 1988, **6**, 655–667.
23 M. P. Singh, G. C. Hill, D. Peoc'h, B. Rayner, J.-L. Imbach and J. W. Lown, *Biochemistry*, 1994, **33**, 10271–10285; Y. Coppel, N. Berthet, C. Coulombeau, C. Coulombeau, J. Garcia and J. Lhomme, *Biochemistry*, 1997, **36**, 4817–4830; S. D. Cline, W. R. Jones, M. P. Stone and N. Osheroff, *Biochemistry*, 1999, **38**, 15500–15507.
24 R. D. Berger and P. H. Bolton, *J. Biol. Chem.*, 1998, **273**, 15565–15573.
25 H. Ide, H. Shimizu, Y. Kimura, S. Sakamoto, K. Makino, M. Glackin, S. S. Wallace, H. Nakamuta, M. Sasaki and N. Sugimoto, *Biochemistry*, 1995, **34**, 6947–6955.
26 C. A. Hunter and J. K. M. Sanders, *J. Am. Chem. Soc.*, 1990, **112**, 5525–5534; E. A. Meyer, R. K. Castellano and F. Diederich, *Angew. Chem., Int. Ed.*, 2003, **42**, 1210–1250; M. O. Sinnokrot, E. F. Valeev and C. D. Sherrill, *J. Am. Chem. Soc.*, 2002, **124**, 10887–10893.
27 M. Ardhammar, T. Kurucsev and B. Nordén, in *Circular Dichroism: Principles and Applications*, ed. N. Berova, K. Nakanishi and R. W. Woody, Wiley-VCH, New York, 2000, pp. 741–768.
28 F. D. Lewis, T. Wu, E. L. Burch, D. M. Bassani, J.-S. Yang, S. Schneider, W. Jaeger and R. L. Letsinger, *J. Am. Chem. Soc.*, 1995, **117**, 8785–8792; J. Cadet and P. Vigny, *Bioorganic Photochemistry*, ed. H. Morisson, 1990, pp. 1–272, John Wiley & Sons, New York.
29 C. R. Cantor and P. R. Schimmel, *Biophysical Chemistry*, W. H. Freeman, New York, 1980.
30 N. Berova and K. Nakanishi, in *Circular Dichroism*, ed. N. Berova, K. Nakanishi and R. W. Woody, Wiley-VCH, New York, 2000.
31 F. D. Lewis, Y. Wu, L. Zhang, X. Zuo, R. T. Hayes and M. R. Wasielewski, *J. Am. Chem. Soc.*, 2004, **126**, 8206–8215.
32 P. Beak and L. Chao, *Tetrahedron*, 1994, **50**, 5999–6004.

 This journal is © The Royal Society of Chemistry 2006